JOURNAL OF SPACECRAFT AND ROCKETS
Vol. 56, No. 1, January–February 2019

Cassini Spacecraft Attitude Control System Performance and Lessons Learned, 1997–2017

Allan Y. Lee* and Thomas A. Burk†
California Institute of Technology, Pasadena, California 91109-8099

DOI: 10.2514/1.A34236

A sophisticated interplanetary spacecraft, Cassini–Huygens was launched on 15 October 1997. After achieving orbit at Saturn in 2004, Cassini collected science data throughout its four-year prime mission (2004–2008) and nine-year extended mission (2008–2017). The Cassini Attitude and Articulation Control Subsystem (AACS) is perhaps the spacecraft subsystem that must satisfy the most mission and science pointing requirements. The performance of the Cassini AACS design was superb from launch through end of mission. All key mission and science requirements were met with significant margins. Overviews of the Cassini attitude control system design and flight performance (in 1997–2017) are given in this paper. Processes taken by the attitude control operations team to guard against human errors are also outlined. Cassini flight experience and many lessons learned are equally applicable to the safe operations of other interplanetary missions.

I. Introduction

THE Cassini spacecraft was launched on 15 October 1997 by a Titan 4B launch vehicle. After an interplanetary cruise of 6.7 years, it arrived at Saturn on 30 June 2004. To save propellant, Cassini made several gravity-assist flybys: two at Venus and one each at Earth and Jupiter. After achieving orbit at Saturn in 2004, Cassini collected science data throughout its four-year prime mission (2004–2008). The first extended mission called the Cassini Equinox Mission was completed in September 2010. The second extended mission called the Cassini Solstice Mission was completed on 15 September 2017. Major science objectives of the Cassini mission included investigations of the configuration and dynamics of Saturn's magnetosphere, the structure and composition of the rings, the characterization of several of Saturn's icy satellites, and Titan's atmosphere constituent abundance [1].

Cassini carried 12 scientific instruments. Six instruments measured properties of objects remote from the spacecraft. An example was the imaging science subsystem with a wide and a narrow-angle camera. Cassini also carried six instruments that observe fields, particles, and plasma waves. An example of these instruments was the Ion and Neutral Mass Spectrometer (INMS). INMS was used to determine the chemical, elemental, and isotopic composition of the gaseous and volatile components of the neutral particles and the low-energy ions in Titan's atmosphere and ionosphere. In 2005, Cassini completed three flybys of Enceladus, a small icy satellite of Saturn. Observations made during these flybys confirmed the existence of watery geysers in the South polar region of Enceladus. The discovery of these watery geysers was an important and unexpected discovery made by Cassini [2]. The Cassini mission ended on 15 September 2017, with the plunge into Saturn's atmosphere after 22 proximal orbits with periapsis between the rings and Saturn's cloud tops. This 22-orbit grand finale was stunningly successful [3–5], and the science gathered has led to the rewriting of the textbook of Saturn. In this paper, an overview of the Cassini attitude control system design is given in Sec. II. Key lessons learned are given in Secs. III–XVI. Conclusions are given in Sec. XVII.

II. Overview of Cassini Attitude and Articulation Control Subsystem

Perhaps no other spacecraft subsystem had to satisfy as many science and mission requirements as the Cassini Attitude and Articulation Control Subsystem (AACS) [1]. The Cassini AACS estimated and controlled the attitude of the three-axis stabilized spacecraft. It responded to ground-commanded pointing goals for the spacecraft's science instruments and communication antennas with respect to targets of interest. The AACS also executed ground-commanded spacecraft velocity changes. Table 1 lists the key accuracy requirements of the Cassini spacecraft.

To achieve a high degree of maneuverability and to facilitate high-resolution imaging, Cassini was designed as a three-axis stabilized spacecraft. Attitude determination sensors included two stellar reference units (prime and backup, star tracker) [6,7], two-degree-of-freedom (2-DOF) sun sensors (SSA, prime and backup) [8], two inertial reference unit (IRU, prime and backup) [9–11], and a 1-DOF accelerometer [12]. Attitude control actuators included three fixed reaction wheel assemblies (RWAs) and another RWA that was mounted on an articulable platform [13], two 445 N bipropellant rocket engines (prime and backup), two sets of 2-DOF engine gimbal actuators (prime and backup), and two sets of eight 1 N monopropellant thrusters (blowdown, prime and backup) [14,15]. The locations of this attitude control and propulsion equipment on the spacecraft are given in [1].

AACS acquired stellar reference by first locating the sun using the sun position knowledge from SSA [7] and then sun-pointing the high-gain antenna (HGA) at the sun. The front end of the Cassini attitude estimator was a prefilter that combined multiple star updates into one "composite" star update. These composite star updates were sent to the attitude estimator (an extended Kalman–Bucy filter) every 1–5 s. In between star updates, the spacecraft's attitude was propagated using IRU data. Once attitude was initialized, the AACS maintained knowledge of the spacecraft attitude in a "J2000" celestial coordinate frame. This frame is defined by the Earth mean equator and equinox at the year 2000 epoch. Overall, the in-flight attitude estimator performance was excellent. Details of the Cassini attitude estimator design are given in [16,17]. Postlaunch, representative value of the 1σ attitude estimation error about the tracker's twist axis (spacecraft's X axis) was 12 μrad [1]. Estimation errors about the other two axes were 3 μrad each.

During tour, Saturn, its rings, and its satellites sometime entered the star tracker's field of view (FOV). The presence of one or more of these bright (or extended) objects affected the nominal operation of the star identification (SID) algorithm [16,17]. To deal with this, the

Presented as Paper 2018-2109 at the AIAA SciTech, Guidance, Navigation, and Control Conference, Kissimmee, FL, 8–12 January 2018; received 1 March 2018; revision received 24 May 2018; accepted for publication 9 August 2018; published online 9 November 2018.

*Section Staff, Guidance and Control Section, Division of Autonomous Systems, Jet Propulsion Laboratory, Mail Stop 198-235, 4800 Oak Grove Drive; Allan.Y.Lee@jpl.nasa.gov.

†Cassini Attitude and Articulation Control Subsystem Lead Engineer, Guidance and Control Section, Division of Autonomous Systems, Jet Propulsion Laboratory, Mail Stop 198-235, 4800 Oak Grove Drive; Thomas.A.Burk@jpl.nasa.gov.

Table 1 Key Cassini accuracy requirements [1]

Pointing, pointing stability, and execution accuracies	Requirements
High-gain antenna (HGA) pointing control requirement (radial 99%)	
X-band (telecommunications)	3.2 mrad
Ka-band (radio science)	2.0 mrad
Ku-band (radar mapping of Titan)	4.6 mrad
S-band (Huygens probe relay tracking)	6.0 mrad
Science inertial pointing requirements (radial 99%)	
Control	2.0 mrad
Knowledge	1.0 mrad
Pointing stability requirements (2σ per axis)	
0.5, 1 s	4, 8 μrad
5, 22 s, others	36,100 μrad, others
Gimbaled engine ΔV burns (1σ per axis)	
Fixed magnitude, fixed pointing	10, 17.5 mm/s
Proportional magnitude, proportional pointing	0.35%, 10 mrad
Thruster ΔV burns (1σ per axis)	
Fixed magnitude, fixed pointing	3.5, 3.5 mm/s
Proportional magnitude, proportional pointing	2%, 12 mrad

SID algorithm had to be temporarily "suspended" via ground AACS command. While SID was suspended, the spacecraft (S/C) attitude was propagated using only data from the gyroscopes. Both the prime and backup star trackers and both inertial reference units were calibrated by the AACS operations team periodically [10,11].

During early cruise, Cassini used a set of eight 1 N monopropellant reaction control system (RCS) thrusters to maintain the spacecraft attitude about all axes. Four Y-facing thrusters formed two thruster couples to control the S/C's Z-axis attitude. Another four Z-facing thrusters were used to control both the S/C's X and Y-axis attitude. A bang–bang (BB) thruster control algorithm was used by Cassini AACS. It used error signals that were weighted sums of per-axis attitude control errors and attitude rate control errors to control thruster firings [17]. However, such a control algorithm can result in "two-sided" limit cycles that could waste both hydrazine and thruster on/off cycle. To counter these drawbacks, the Cassini's BB controller incorporated a "self-learning" feature to produce, as much as possible, "one-sided" limit cycles in the presence of small solar torque. The resultant one-sided limit cycles saved both hydrazine and thrusters' on/off cycles [1,17]. Details are given in Sec. III. Thrusters were also used to detumble the spacecraft after it was released from the launch vehicle, to control the spacecraft's attitude during low-altitude Titan flybys, to bias the RWA's angular momenta, and to execute small ΔV burns.

The RWAs were used primarily for S/C attitude control when precise and stable pointing of a science instrument (such as the narrow-angle camera) was required during the prime mission phase. The basic structure of the Cassini RWA controller was a decoupled, three-axis, proportional and derivative (PD) controller [18]. However, because of the presence of RWA bearing drag torque, a PD controller would not be able to drive the spacecraft attitude control error to zero unless an integral term was added to the controller. This was overcome by the addition of a proportional and integral estimator of the RWA frictional torque. In effect, integral control action was added "locally" to remove any steady-state attitude control errors [18]. The merit of this control architecture is given in Sec. IV.

During the tour phase, the spacecraft pointing stability performance achieved with the RWA control system was superb. Details are given in Sec. V. However, the use of reaction wheels was subjected to three operational constraints. First, the spin rates of all RWA must not exceed the angular momentum capacity of the wheels. Second, for RWA health reason, the total number of revolutions the RWA incurred as a result of performing science slews must be kept as low as possible. These two constraints discouraged high-speed wheel operations. Third, the operational hours the wheels spent inside a "low-rpm" region must be minimized. This was because, below a certain spin rate, the thickness of the lubrication film (between the bearing balls and races) would be smaller than the rms value of the surface roughness of the balls and races. This would lead to metal-to-metal contact between these bearing elements, which was highly undesirable. Many spacecraft with attitude controlled by reaction wheels had encountered bearing-related flight anomalies. In anticipation of the need to maintain good RWA health for a long mission, the Cassini AACS team developed and used a ground software tool named Reaction Wheel Bias Optimization Tool (RBOT) [19]. Details are given in Sec. VII.

For navigation purposes, the Cassini interplanetary mission required both large and small trajectory correction maneuvers. Trajectory corrections performed before Saturn orbit insertion (SOI) were called trajectory correction maneuvers (TCMs). After SOI, they were called orbit trim maneuvers (OTMs). Large burns (with magnitude greater than 0.25 m/s) were performed by a rocket engine [20–22]. During a main engine burn, the X and Y axes of the spacecraft's attitude were controlled by the engine gimbal actuators using a thrust vector control (TVC) algorithm [20,21]. Concurrently, four Y-facing thrusters were used to control the spacecraft's Z-axis attitude. The ΔV imparted on the spacecraft was estimated by an accelerometer (ACC). Because the ACC's bias changes slightly from burn to burn, it was calibrated before the start of each and every main engine burn. The flight software (FSW) used the calibrated bias to accurately determine the magnitude of the ΔV imparted on the spacecraft. Each burn was terminated once the commanded ΔV magnitude was achieved. Flight performance of the TVC algorithm was excellent [1,22–24]. See also Sec. IX.

Cassini used four Z-facing thrusters to execute small ΔV burns (they are called RCS burns) [23,24]. During a RCS burn, the Z-facing thrusters were fired to achieve the ΔV. Engine off-pulsing was needed to negate the self-induced disturbance torque caused by the S/C's c.m. offset (from the Z axis). Also, misaligned Z-facing thrusters generated a small disturbance torque about the S/C's Z axis. Four Y-facing thrusters were fired to maintain the spacecraft's Z-axis attitude. See also Sec. X.

During the cruise phase (from launch on 15 October 1997 to the start of the approach science phase on 1 January 2004), thrusters were used to roll and yaw the spacecraft attitude to align the preaimed rocket engine with the target ΔV vector. "Settling" times on the order of 5 min were "inserted" in between the roll and yaw turns and in between the end of the yaw turn and the start of the burn. Settling times provided time for the sloshing motion of propellant in tanks to be damped out before engine ignition. Once a burn was completed, the spacecraft would "unyaw" and "unroll" back to its initial attitude. Again, settling times were inserted between these "unwind" turns. These thruster-based slews imparted unwanted ΔV on the spacecraft. Even though the magnitudes of these ΔV were predicted, they still, in a small way, affected the accuracy of the burn. To improve burn accuracy and to save valuable hydrazine, beginning with TCM-18 (in April 2002 [23]), both the roll and unroll turns were executed using a set of reaction wheels. See also Sec. VIII.

Pointing the Cassini spacecraft involved commands to turn to and track targets of interest. On Cassini, pointing commands referenced celestial objects themselves. If the target was Saturn, a single command caused the spacecraft to turn to Saturn. Once there, the spacecraft tracked Saturn until commanded to turn to another object. This means that target motion compensation was inherent in the design. With more than a dozen science instrument boresights, Cassini pointing commands referenced the name of the science instrument boresight itself as the object to point at Saturn. Cassini was able to explicitly point boresights at celestial objects by use of an innovative pointing model called inertial vector propagator (IVP) [25]. IVP provided a remarkably robust yet structured process that took advantage of powerful onboard vector propagation algorithms combined with sophisticated targeting options that science teams took full advantage of on the ground [26].

Pointing the Cassini spacecraft was achieved using two "inertial" vectors and two "body" vectors to command a unique inertial attitude in space. The fundamental requirement was to point a selected primary body vector at a primary inertial vector object. For example, during data playback to Earth, the primary pointing was commanded to be "XBAND" to "EARTH". Here, XBAND was the radio-frequency

boresight vector of the antenna, and the EARTH was the head of an inertial vector from the spacecraft to Earth. To establish a complete three-axis inertial attitude, a secondary pair of body and inertial vectors was also specified. For example, a secondary pair could be "NAC" to "SATURN", where NAC was the narrow-angle camera boresight body vector and Saturn was the time-varying inertial vector from the spacecraft to the center of Saturn. The primary pointing was always achieved, whereas the angle between the secondary pair was minimized given the constraint that the primary vectors must be collinear.

Inertial vectors resided in an onboard inertial vector table that was populated by ground IVP commands. A ground IVP tool was loaded with the desired pointing sequence and with up-to-date spacecraft and celestial body ephemeris and physical constants files. The tool "fit" inertial vectors to approximate the ephemeris using either conic or Chebyshev polynomial coefficients. Conic coefficients were just position, velocity, and a gravity parameter. Conic propagation involved solving Kepler's equation [27]. Conics propagate accurately when there is a dominant central body (for Cassini, the dominant body was Saturn). Because conics do not always suffice, Chebyshev polynomial vectors (of up to 12th order) were also used by IVP [28]. Polynomials were used during transitional periods in the spacecraft's trajectory as gravitational dominance shifted from Saturn to Titan, for example. Conic and polynomial vector fits were done on the ground using the IVP tool to an accuracy of 40 μrad.

For Cassini AACS, two aspects of pointing commands were checked by the constraint monitor (CMT) flight software object before they were passed to the attitude controller [29]. First, the per-axis slew rates and accelerations were checked against sets of rate and acceleration limits that represented the capability of the thrusters (or a set of reaction wheels). Any per-axis rates or accelerations that were higher than their CMT threshold were "limited" by the CMT. Only the slew command limited by these "dynamic" constraints was implemented by the attitude controller. CMT also checked "geometric" constraints to make sure that the angle between a specific body vector and an inertial vector (usually the sun-line vector) was larger than a preselected threshold. For example, the boresight vector of the narrow-angle camera must not be closer than 12 deg relative to the sun-line vector (actually, any part of the sun). The commanded S/C attitude was altered by the CMT if a geometric constraint violation was anticipated by the CMT. See also Sec. XI.

There were two fundamental Cassini AACS fault protection (FP) requirements [30–35]. First, during all mission phases, the spacecraft must be able to "fail safe" by autonomously locating and isolating any single failure, recovering to a thermally safe and commandable attitude, and then waiting for further instructions from the ground operators. In 20 years of flight operations, the Cassini spacecraft entered "safe" mode a total of six times. Details are given in Sec. XIV. Second, during a few time-critical events (such as the SOI [22,36] and probe relay [37] sequences), the spacecraft could not afford to simply isolate a failure and wait for ground instruction. In these "time-critical" events, the spacecraft had to "fail operational" by autonomously recovering to a much larger set of its capabilities and then proceed with a previously uplinked "critical" command sequence. Note that the ground-generated critical command sequence was an integral part of Cassin's "fail operational" capability. Following an autonomously detected failure in the critical sequence, the command data system (CDS) temporarily suspended the critical sequence, coordinated an autonomous fail-safe response, and then restarted the critical sequence from the last achieved "checkpoint". Each critical sequence had several checkpoints, each of which enforced any necessary differences between the fail-safe configuration and the operational configuration for subsequent critical sequence activities. Operational aspects of the Cassini AACS FP design are described in Sec. XIII.

Prelaunch, many engineers worked on the designs and testing of AACS hardware and software. Knowledge of the limitations of the attitude control subsystem were recorded and passed to the mission operations team to ensure spacecraft safety [38]. One efficient way that knowledge was transferred from the design and test teams was to write "flight rules" that the operations team followed during mission operations. The rationales behind the needs to enforce these rules must be clearly stated. Approved flight rules could be enforced via ground software, manual inspection, or by other means. Flight rules were enforced until they were no longer applicable. For example, launch-related flight rules were removed after the launch event. On the other hand, new flight rules were written to incorporate lessons learned from flight experience gained via mission operations. See also Sec. XII.

One of the major science objectives of the Cassini mission was an investigation of Titan's atmosphere constituent abundance. To this end, the instrument ion and neutral mass spectrometer (INMS) played a key role [1,39]. Postlaunch, the AACS team devised methodologies to estimate Titan and Enceladus atmospheric densities using RCS thruster and/or RWA data collected during low-altitude flybys of these moons. Details of these methodologies are described in Sec. XVI. These AACS-centric density estimates were used to calibrate and supplement density estimated using INMS [39].

III. In-Flight Tuning of Reaction Control System Attitude Controller's Parameters

After crossing 2.5 A.U. from the sun, ground communication with the Cassini spacecraft was switched from Low Gain Antenna (LGA) to HGA. This required tightening the RCS controller deadband (DB) from [20, 20, 20] to [2, 2, 20] mrad about the S/C's X, Y, and Z axes, respectively. This new deadband significantly increased the consumption rates of two thruster consumables: the thrusters' on/off cycle and the hydrazine. Following the completion of the inner solar cruise phase, the flight team tuned the RCS controller parameters to conserve these consumables ahead of the long outer solar cruise phase.

During periods when fast changes in S/C attitude were not required, the RCS controller reverted from the conventional BB control algorithm (also called the "high rate" mode) to the adaptive pulse width adjuster mode (APWA, also known as "low rate" mode). The APWA logic was used to tune the thruster on time based on the current and previous limit-cycle peak magnitudes (as denoted by "L", in units of radians, in Fig. 1) and used the previous thruster on time to determine the desired on time for the next thruster pulse. That is, the next thruster on time was the last thruster on time multiplied by a factor computed by: $[\sqrt{L_2} + \sqrt{L_3}]/[\sqrt{L_1} + \sqrt{L_2}]$. Here, L_1 and L_2 are the spacecraft angular excursions traveled by two previous one-sided deadband excursions, and L_3 is the target excursion of the next cycle (see Fig. 1). With this logic, if L_1 is smaller than L_3, then the multiplication factor is larger than 1, and the next pulse width will be larger than the last pulse width, and vice versa. After a few "training" cycles, APWA will converge to the desired limit cycle [17]. The size of L_3 was selected to achieve an angular excursion that was as large as possible but without "touching" the deadband boundary. The benefit of using APWA was to reduce the number of two-sided deadband firings and thereby reduce the average hydrazine consumption rate.

Two in-flight tunings were performed to determine the optimal values of two APWA parameters: P_1 and P_2. The first test was

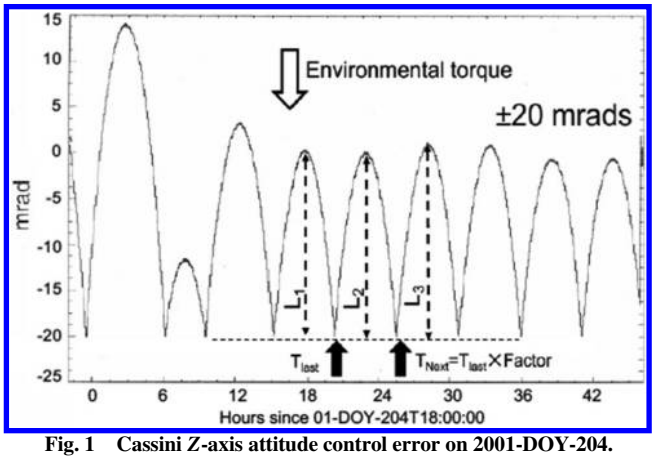

Fig. 1 Cassini Z-axis attitude control error on 2001-DOY-204.

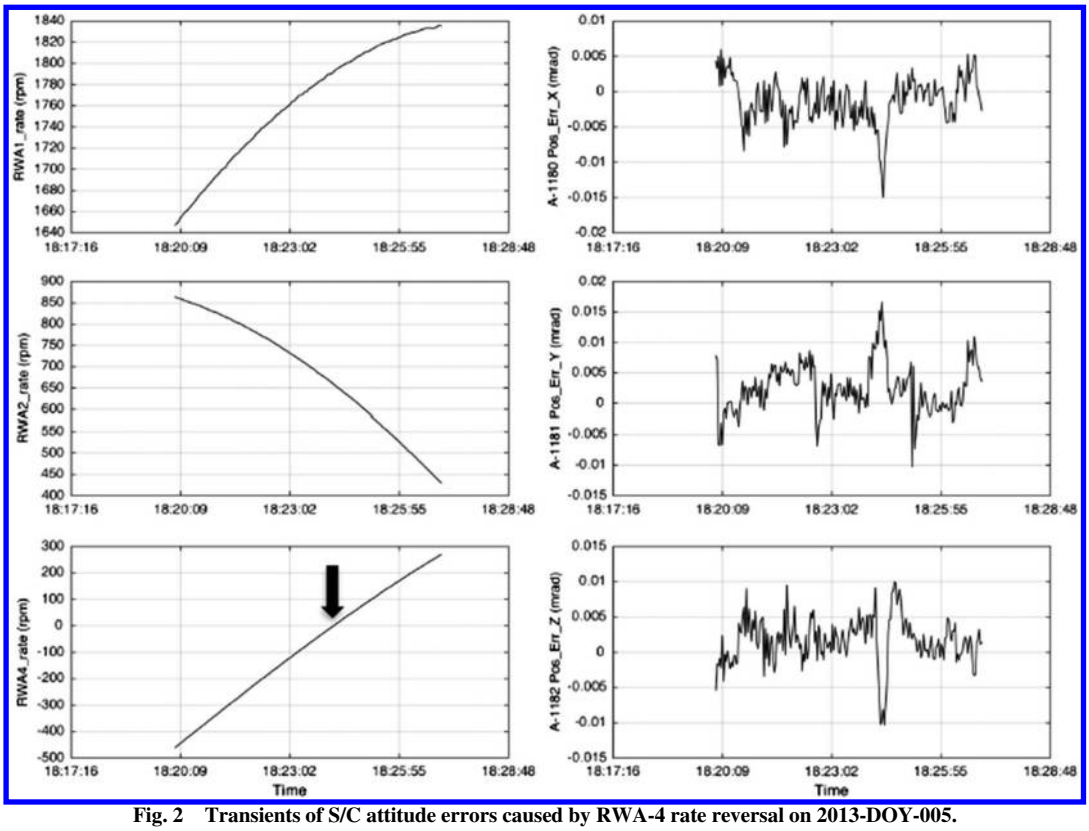

Fig. 2 Transients of S/C attitude errors caused by RWA-4 rate reversal on 2013-DOY-005.

performed from 2001-DOY-140 to 2001-DOY-144 with the P_1 changed from 120 to 200 μrad. The second test was performed from 2001-DOY-203 to 2001-DOY-206 with P_2 changed from $\sqrt{0.75}$ to $\sqrt{0.5}$. Test results were analyzed by both the attitude control and propulsion teams. Their analyses of data from the first test indicated a 19.3% reduction in the consumption rate of the thrusters' on/off cycles. For the second test, a 41% reduction in the hydrazine consumption was found [1,14]. Based on these positive flight results, these new parameter values were made permanent in the AACS flight software.

The Cassini RCS controller design also had logic to autonomously switch between the "high-rate" and "low-rate" RCS control modes. This high-to-low mode switch was performed if both the rate command and rate error signal were persistently low (less than 0.05 mrad/s) for a period of time T_{switch}. Based on results of simulation performed prelaunch, T_{switch} was selected to be 10 min. Postlaunch, T_{switch} was lengthened to 40 min, resulting in reductions in the consumption rates of both propellant and thruster on/off cycle. This is another example of the need to revisit the values of controller parameters selected prelaunch, which were often selected without good knowledge of the environmental torque imparted on the spacecraft. Cassini experience indicates that, for missions with RCS thrusters having small minimum impulse bit, the RCS controller should be designed with an APWA-like logic to achieve single-sided deadbanding. Via in-flight tuning, the logic could significantly reduce the consumption rates of thruster consumables during the long RCS-controlled cruise phase of the mission [40].

IV. Reaction Wheel Assembly Controller Design and Bearing Drag Torque Estimator

The reaction wheel assemblies were used primarily for attitude control when precise and stable pointing of a science instrument was required during the prime mission phase. The RWA controller consisted of a bearing drag torque estimator in the FSW. With this drag torque compensation system, regardless of whether the bearing drag torque was at its nominal level or was elevated due to anomalous bearing performance, the appropriately compensated motor torque command was sent. As a result, impacts of the bearing drag on the S/C attitude control performance were minimized. This is one key reason why the Cassini pointing stability requirements were met with large margins as mentioned in the following section.

For Cassini, the drag torque estimator was designed to accurately track the bearing drag torque only in the steady state. When the physical drag torque changed due to, for example, a spin rate reversal ("zero-crossing"), the drag estimator could still track the physical drag torque but there would be transient tracking error. The faster the drag torque changes, the larger the tracking error would be [13]. As a result, the drag torque estimator would not be able to fully compensate for the physical drag, and the spacecraft attitude control and stability performance would suffer as a result. As an example, as depicted in Fig. 2, there was a zero crossing of the RWA-4 rate at 2013-DOY-005T18:24:11 (as indicated by a bold arrow head). As a result of the incomplete RWA-4 drag torque compensation, noticeable perturbations of all three per-axis S/C's attitude control errors were observed soon after that rate reversal event. For Cassini, this was not a problem because of the large performance margin (see the following section) and the transient nature of the performance degradation. However, for missions without the benefit of large performance margin, a more capable drag torque estimator that can better track transient drag "spikes" would be needed.

Since the year 2000, all Cassini RWA bearings experienced a class of anomalous drag torque that was generally "spiky" in nature [13]. The drag spikes usually occurred at a time when the RWA was maintained at a constant spin rate for a long period of time. In this condition, the expected level of RWA bearing drag torque was nearly constant. However, drag torque spikes were often observed superimposed on the "constant" drag torque. The initial sudden rise in drag torque was often followed by either a rapid (several minutes) or gradual (several hours) exponential decay to the nominal drag level. The spikes had a wide range of magnitudes, and they occurred in a wide range of RWA spin rate conditions [13]. A representative set of these RWA drag spikes is given in Fig. 3. The definite cause of these drag torque spikes is unknown. It is our conjecture that it is an "oil jog" phenomenon: a rapid incorporation of a small amount of lubricant by the bearings followed by its relatively slow dispersal.

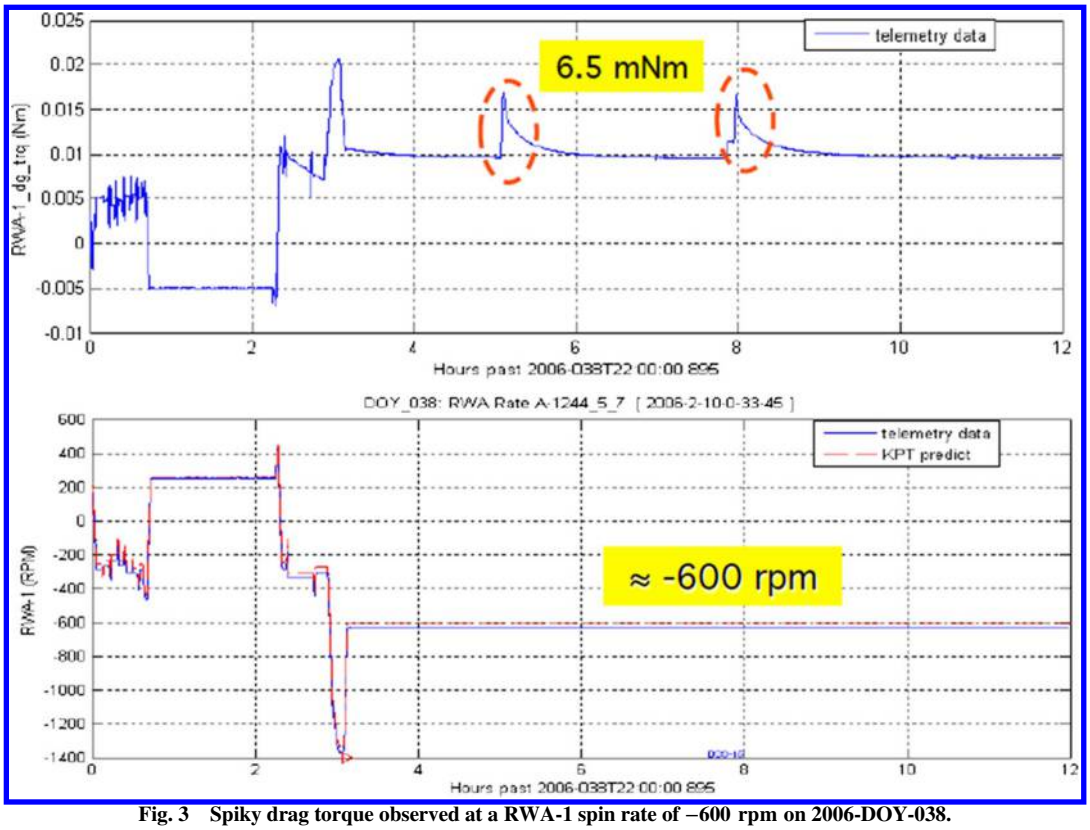

Fig. 3 Spiky drag torque observed at a RWA-1 spin rate of −600 rpm on 2006-DOY-038.

Bearings can have small pockets of lubricant that collect outside of the normal ball/cage and ball/race contact areas. They can become entrained in the contact areas by a variety of processes. Bearings that suddenly encounter an addition of oil will show an abrupt increase in drag that will then dissipate. The size of the drag torque spike and the time required to redistribute the oil depend on the amount of oil in question and the RWA spin rate at the time the spike occurred [13]. Again, the implemented Cassini RWA drag torque estimator could not fully compensate for these drag spikes, and the spacecraft attitude control and stability performance degraded slightly if the drag spikes were large. This is another reason to consider more capable drag torque estimators such as those mentioned in [41].

V. Spacecraft Pointing Control and Stability Performance

Spacecraft pointing control error is defined by the angle between the actual pointing direction and the desired pointing direction of a specific onboard body vector. The spacecraft pointing-control requirement was driven by the need to guarantee that the selected science target falls inside the FOV of the science instrument. If the 2 mrad (radial 99%) pointing control requirement (see Table 1) for NAC was met, the captured image was guaranteed to fall inside the 6.1×6.1 mrad FOV of the NAC. In flight, both the inertial pointing-control and pointing-knowledge requirements were met with margins [42].

Spacecraft pointing stability is defined by the angle variation of the actual pointing direction of an onboard body vector over a time duration called "exposure time". The mathematical definition of the Cassini pointing stability performance metric was defined in [43]. The spacecraft pointing stability requirement was driven by the need to ascertain that, over the exposure time of the imaging, incoming photons were "focused" on the intended set of camera charge-coupled device pixels (see Table 1 [42]). Sources of jitter inherent to the Cassini spacecraft include the reaction wheels' static and dynamic imbalances, RWA bearing drag torque, and disturbance torque generated by sloshing motion of propellants in their tanks. Attitude determination sensor noise with a significant frequency content within the controller bandwidth looks like valid "commands" to the attitude controller. Accordingly, the controller generates control torque to cause the spacecraft attitude to follow these erroneous commands. This results in undesired spacecraft vibration.

The dependency of the spacecraft pointing stability performance on exposure time, in log-log scale, is depicted in Fig. 4. These results overwhelmingly confirm that the Cassini pointing stability requirements were met with very significant margin. The quality of images returned by the high-resolution cameras provided ample evidence of this claim.

VI. Impacts of Reaction Wheel Assembly Induced Microphonic on Science Instruments

The Composite Infrared Spectrometer (CIRS) was one of the key Cassini remote sensing science instruments. It captured infrared light and split the light into its component wavelengths. It then measured the strength of the light at each of those wavelengths primarily to

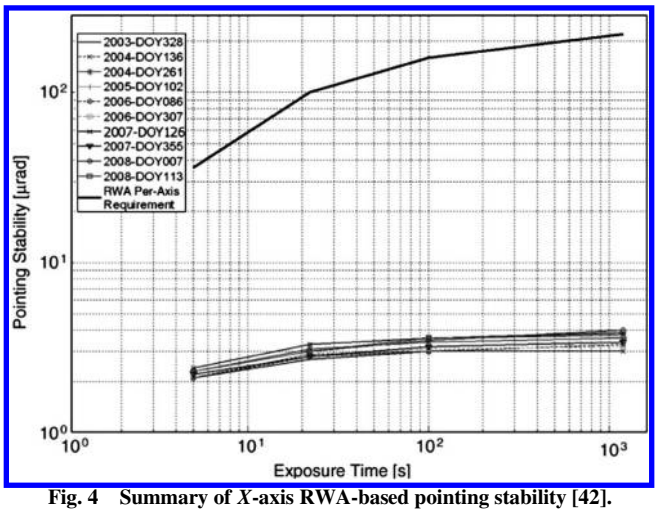

Fig. 4 Summary of *X*-axis RWA-based pointing stability [42].

measure the temperature of objects but also their composition. The scan mechanism subassembly of CIRS was used to maintain its scanning mirror at a constant scan velocity. Strong external disturbances at the CIRS base plate can cause large scan velocity variations that disrupt the regular sampling process. This resulted in too many samples in the CIRS interferogram (raw data) that degraded the CIRS data. A key disturbance force came from the static and dynamic imbalances of the three spinning reaction wheels. There were other microphonic sources on the spacecraft, but only the reaction wheels could not be powered off at the time of CIRS operations.

Prelaunch, the impact of spacecraft vibrations on CIRS operations was a concern. Workshops on the S/C microphonic environment were conducted to address this concern. To evaluate the impact RWA-induced vibrations have on the CIRS operation, three sets of data were examined: 1) the measured excitation force of the RWA over a range of spin rates, 2) the measured transfer function between the RWA force and the CIRS base-plate motion, and 3) the sensitivity of the CIRS scan velocity error due to the base plate movement. In addition to these component-level measurements, the end-to-end RWA-to-CIRS measurements had also been determined on the spacecraft.

In flight, CIRS calibration data were found to be impacted by disturbances generated by the RWA. This was the case in spite of the fact that the static and dynamic imbalances of the reaction wheels were at least a factor of 3 smaller (that is, better) than their respective requirements. Correlation analyses between the RWA's spin rate and the fraction of good CIRS calibration data indicated that when the RWA operated at high rotation frequency (greater than 1300 rpm), calibration data loss became significant. Multiple options were explored to mitigate this problem (see [44]). These remedial options provided up to about 70–80% return of the CIRS calibration data, partially compensating for this microphonic problem. Missions with science instruments whose operations are sensitive to vibrations should pay attention to microphonic generated by RWA imbalances. Prelaunch, the evaluation of the RWA-to-instrument microphonic impact should be performed conservatively.

VII. Reaction Wheel Bias Optimization Tool

In preparation for the extensive use of reaction wheels in the prime mission (which started on 1 July 2004), the operations team began to develop a ground software tool named RBOT in early 2001 [19]. Given the time histories of the spacecraft's attitude and attitude rate commands to support science slews from the start to the end of an RWA biasing time segment, RBOT selected a set of optimal biasing rates for the three prime RWA that minimizes a cost function. The cost function was designed to enforce the operational constraints described in Sec. II (see also [19] for the definition of this function). However, for biasing segments with very complex science observations, it was possible that even the best set of RWA bias rates might still contain prolonged periods of spin rate dwelling inside the sub-Elasto-Hydro-Dynamic (EHD) region. In this situation, one of the following two remedial actions was used. The problematic biasing segment could be divided into two or more shorter segments. Alternatively, one could modify some problematic science observation sequence designs (e.g., slew the S/C using a set of slower rate and/or acceleration profile limits) to allow RBOT to find solutions without long dwelling inside the sub-EHD region. Disciplined and long-term use of RBOT led to a significant reduction in the daily hours the wheels spent in the sub-EHD region. For example, the per-wheel daily low-rpm duration was 2.5 h in 2005–2006. By 2010–2013, it was reduced to 0.35 h. This drop in the time duration the wheels spent in the sub-EHD region has benefitted the health of the wheels.

Many spacecraft with attitude controlled by reaction wheels had encountered bearing-related flight anomalies. Over the years 1997–2017, the Cassini mission control team learned many useful RWA-related lessons [41,45–48] and they are summarized in [13]. Some of these lessons are equally applicable in protecting the health and safety of RWAs on other spacecraft. In conclusion, attitude control reaction wheels must be managed with great care.

VIII. Estimation of Unwanted ΔV Generated by Thruster Firings

RCS thrusters were used to perform many AACS functions throughout the Cassini mission [1]. Examples of these functions, mentioned in Sec. II, were the executions of small ΔV burns and RWA biasing. During these activities, Y-facing thrusters were always fired in pairs. Hence, the forces generated by these Y-facing thrusters canceled each other, and the ΔV imparted on the spacecraft was negligible. On the other hand, the firings of Z-facing thrusters generated unwanted ΔV on the spacecraft because they all point in the same $-Z$ axis direction. These unwanted ΔV impacted the spacecraft flight path and had to be predicted by the attitude control team for the navigation team.

The linear momenta imparted on the spacecraft due to the firings of the Z-facing thrusters were estimated using the estimated value of the thruster magnitude and the commanded on time of the four Z-facing thrusters. However, thrusters do not respond "instantaneously" to their firing commands. Thruster dynamics were modeled with exponential "rise" and "fall" time constants. The Cassini AACS flight software used the calibrated magnitudes of the thrusters' magnitudes [49,50], rise/fall time constants [15], and the estimated mass of the spacecraft [14] to estimate the unwanted ΔV. These parameters were routinely updated via ground command based on maneuver navigation reconstruction. The estimated thruster magnitudes were also trended to monitor the health of the thrusters [12,50].

In flight, the AACS team used a ground software tool named Kinematic Prediction Tool (KPT) to automate the prediction of ΔV (see also Sec. XI). The AACS team also used the simulation test bed Flight Software Development System (FSDS) to predict the ΔV imparted on the S/C due to RWA biasing events, RWA drag torque characterization tests, as well as during low-altitude Titan flybys [51–53]. The ΔV magnitudes predicted by the FSDS were typically more accurate than those predicted by KPT because individual attitude control thruster firings were accounted for in FSDS-based simulation (but not so in KPT). The requirement on the ΔV prediction accuracy, as imposed by the navigation team on the AACS team, was $\leq$2.5 mm/s per activity. In flight, this ΔV prediction accuracy was usually met with margin. But the requirement was violated several times due to ground software prediction limitations and one time due to a human error. Details of these ΔV prediction errors are given in [44]. During the tour phase (from the end of the SOI burn to the start of the proximal orbits phase in 23 April 2017) of the Cassini mission, to gain visibility of the actual ΔV imparted on the spacecraft, ΔV telemetry was downlinked with resolution of 0.04 mm/s per data number [54].

If RWA biasing events are performed using only couples formed by Y-facing thrusters, the resultant ΔV will be near zero. In this case, accurate prediction of the unwanted ΔV becomes unnecessary. This advantageous approach was anticipated prelaunch. However, during the early phase of the Cassini mission, the navigation team preferred to have the S/C in an Earth-pointed attitude during RWA biasing events (radiometric tracking will provide visibility of the unwanted ΔV). Thus, RWA biasing by Y-facing thrusters alone was not possible during the early years at Saturn. In the later part of the mission, RWA biasing events were performed without this Earth-pointed attitude constraint. Using the revised RWA biasing approach, called "Y-biasing" [55], the ΔV generated was almost zero, and the propellant consumption was also smaller than its counterpart in the Earth-pointed RWA biasing event.

IX. Engine-Based ΔV Control and Operational Issues

Delta-V maneuver performance on Cassini was outstanding. Since launch, 360 maneuvers (183 Main Engine (ME) ΔV and 177 RCS ΔV) were executed. The NASA Deep Space Network (DSN) support was excellent; not a single maneuver was missed, and maneuver telemetry playback was excellent. Maneuver design always included a nominal (prime) design and a backup design. The backup would be performed if the prime maneuver did not execute, or very rarely, if there was a compelling navigation or operations reason why the backup maneuver was preferable. The backup was typically

scheduled 24 h after the prime maneuver. A typical maneuver DSN pass was 9 h in duration with burn ignition planned 6 h into the track. DSN maneuver tracks were scheduled in pairs: a 9 h track for the prime, followed 24 h later by a 9 h backup track. A maneuver sequence was typically uplinked during the DSN track in which it would execute. This let the ground team use the most up-to-date navigation data in designing the maneuver. In some cases, if orbit determination was stable and there was a significant ΔV penalty to fall to the backup, it was desirable to uplink the prime maneuver one or two days ahead of its execution time. This maximizes the chance of doing the prime maneuver and ensured that bad weather at a DSN station on the day of the maneuver would not affect its nominal execution.

Maneuvers were minisequences that overlayed the Cassini background sequence. The maneuver design process had to be rapid and robust. To achieve this, maneuver sequences were designed as "blocks" of time-ordered commands that were always issued. Most of the design occurs many days ahead of the maneuver, including early estimates by the navigation team of the orbit determination and burn ΔV vector. As the orbit determination was updated with more data, its effect on the maneuver was evaluated and any problems mitigated. A big effort was made to automate as much as possible the design and verification of maneuver sequences. The Maneuver Automation Software (MAS) ground tool was the result of this effort [56]. In less than 30 min, a complete maneuver sequence was designed and verified using MAS [44]. One important lesson from Cassini maneuver design was that, over the course of the mission, a large number of changes occurred that affected the basic design of the maneuver sequence. Had maneuver design and implementation been placed in onboard flight software, this would have caused major problems. Ground tools are much easier to update and validate than flight software.

Burn execution error is a measure of how closely the spacecraft achieves the desired maneuver ΔV. Typically, JPL navigation teams use a linear Gates model to represent maneuver execution error. The ΔV magnitude error is expressed as the sum of a fixed magnitude error, which is independent of the commanded ΔV magnitude, and a proportional magnitude error that is proportional to the commanded ΔV magnitude. The ΔV pointing error is modeled similarly. This approach was used for missions such as Voyagers, Galileo, Magellan, Cassini [20,21], and others. For ME burns, a key sensor on Cassini was the single-axis (spacecraft Z axis) ACC. Accumulated ΔV from this sensor was used for each one of the 183 main engines burns since launch. Each burn cutoff at the targeted ΔV magnitude. A back-up timer, normally set at 5% above the nominal burn duration, was never triggered in flight. The ACC scale factor was key in main engine burn magnitude execution error. Fine adjustments of the scale factor were done on the ground using Doppler-derived execution errors over many in-flight burns, and any adjustment was carefully considered and tested before an onboard update [44]. The Cassini ACC scale factor was updated four times in flight. Overall, the Cassini ACC performance was excellent throughout the 20 years of the Cassini mission [57–59]. Postlaunch, the Cassini ME ΔV execution accuracy (both magnitude and pointing) improved steadily with flight experience [57]. For example, the Gates proportional pointing accuracy of ME burns improved from 10 mrad (1σ, see Table 1) prelaunch to 1 mrad by the time of OTM-326 (after 145 ME ΔV burns). The corresponding Gates proportional magnitude accuracy of ME burns improved from 0.35% (1σ, see Table 1) prelaunch to 0.02% [44,57–59].

X. Thruster-Based ΔV Control and Operational Issues

RCS ΔV maneuvers were performed when the desired ΔV was less than what the main engine system could safely perform. At launch, this ΔV "cutoff" point was chosen to be about 0.5 m/s. The shortest allowable ME burn duration, consistent with hardware requirements, was 1.0 s. The shortest ME burn actually performed was OTM-93 with a 0.27 m/s ΔV and a burn duration of 1.5 s. A complete list of ΔV burn executed by Cassini using either ME or RCS is given in [58].

RCS maneuvers were performed using the four 1 N $-Z$-facing thrusters. During the latter stages of the mission at Saturn, each blowdown thruster produced a force of about 0.6 N. The burn attitude for RCS ΔV maneuvers was defined by aligning the S/C $-Z$ axis with an inertially fixed desired ΔV vector defined by the navigation team. Because the accelerometer was designed for ME burns, the quantization of ACC ΔV measurements was not fine enough (1 ACC count equals about 4.5 N·s of impulse) to allow accurate estimates of ΔV during RCS burns. Instead, a "virtual accelerometer" was used, which estimated thrust acceleration for each firing Z-thruster based on its on/off status, as well as onboard estimates of spacecraft mass and the nominal thrust for each thruster (parameters in the maneuver minisequence). From these quantities, the FSW computed an estimated ΔV for each firing thruster. In an RCS burn, all four Z-axis-facing thrusters were nominally firing together. Burn cutoff was commanded when the accumulated ΔV magnitude reached the target. Without an explicit sensor, RCS burns were essentially "timed" burns where total thruster on time was accumulated. Thus, ΔV magnitude execution error was directly related to the FSW estimates of the thruster forces. Ground tools estimated these forces using tank pressures and other propulsion system data [14], but the best way to keep the onboard settings accurate was to adjust them based on recent navigation (e.g., Doppler) flight data [44].

In 2008, the prime A-branch thrusters experienced significant thrust force degradation, which caused two of the four $-Z$-facing thrusters to permanently lose 25–40% of their nominal thrust. This led to a 5% ΔV underburn during a significant RCS ΔV maneuver. Early in 2009, the ground team switched to the backup B-branch thrusters [60]. The cause of the A-branch degradation is not known definitely [61].

RCS ΔV pointing execution errors were mainly a function of how close Cassini's actual attitude followed the commanded burn attitude during the course of the burn. Cassini turned to the burn attitude using reaction wheels, so the pointing error at burn ignition was essentially zero. Just before ignition, a transition to RCS control occurred, and the burn executed in RCS control while the reaction wheel momentum was held constant throughout the burn. Attitude control deadbands of ± 0.5 deg for the X and Y axes and ± 1 deg for the Z axis limited the maximum attitude control error during and after the RCS burn. Because the center of mass was offset from the spacecraft centerline, four $-Z$ thrusters firing at once induced a torque that caused the attitude error to migrate to one side of the attitude control deadband. When an X or Y deadband was reached, two of the four $-Z$ thrusters pulsed off to provide torque to stop the growth of the attitude control error in that axis. On Cassini, an attitude error integrator was used to avoid unwanted on/off chatter at the attitude control deadband. Details of the integrator performance are described in [44].

Postlaunch, the Cassini RCS ΔV execution accuracy improved steadily with flight experience [44,57–59]. For example, the Gates proportional pointing accuracy of RCS burns improved from 12 mrad (1σ, see Table 1) prelaunch to 4.5 mrad by the time of OTM-328 (after 96 RCS ΔV burns). The corresponding Gates proportional magnitude accuracy of ME burns improved from 2% (1σ, see Table 1) prelaunch to 0.4% [44,57–59].

XI. Ground Simulation and Tools: Keys to Finding Errors

Cassini used a hardware integrated test laboratory for both flight hardware and flight software development and test [51–53,62–64]. Flight spares of many flight hardware components provided outstanding fidelity and made the Cassini ITL an essential operational tool after launch. When combined with robust ground support equipment, the Cassini ITL was the perfect platform to test to-be-flown command sequences. The input products to ITL should be the actual products to be uplinked, where possible. The ground telemetry system was fully integrated into ITL so that ground operators got a preview of their visibility of the actual activities on the spacecraft. The Cassini team tested all critical and first-time events in ITL. ITL telemetry was easily accessible both during and after each test. ITL allowed access to environment "truth" simulation parameters as well as FSW memory

locations and telemetry. Besides telemetry, standard ITL output products included fault protection event logs and records of detailed inputs used in simulation initialization.

Cassini always scheduled ITL procedure walkthroughs so that both the ITL test team and the flight operations team had a common reference to follow for test initialization. Test initialization was important because an effective test must match the states of the spacecraft. Review of the test results was a team responsibility and must be done with great care. A test not carefully evaluated provides little value added. The ITL was also a great resource for in-flight anomaly evaluation, too.

To supplement the ITL, the Flight Software Development System (FSDS) was an "all software" simulator that was used to build and check out the flight software prelaunch [51–53]. It was used extensively in operations because it contained all the flight software, ran faster than real time, and ran on an analyst's workstation. FSDS was used for detailed anomaly or engineering investigations, OTM testing, hardware-related fault insertion, and flight software development and regression testing. FSDS also contained updated models of Saturn and Titan atmospheres and Enceladus plume models. A key aspect of operational success on Cassini was the careful design of test cases. Testing that emphasizes actual operational scenarios was especially valuable [65].

Ground software (GSW) and procedures were used to verify command sequences, check flight rules, design science observations, and design ΔV maneuvers and other engineering activities. They were imperative for ensuring that errors do not get into uplinkable products and ultimately to the spacecraft. It cannot be emphasized enough that directing resources to GSW throughout the lifetime of a mission is key to safe operations. Over 200,000 spacecraft turns to point Cassini to accomplish science observations occurred during the mission at Saturn. All of these slews were designed by the science teams themselves. Integrating all these activities together and ensuring that they meet all applicable flight rules and constraints required robust GSW that both science observation designers and the engineering operations team used.

The bulk of ground software development on Cassini occurred prelaunch and during the 6.7 year cruise from Earth to Saturn. Two key AACS ground software tools were the IVP tool and the Kinematic Predictor Tool (KPT). IVP generated all the fixed and time-varying vector commands that populated the onboard inertial and body vector tables during sequence execution [26]. The KPT processed all the pointing-relating commands in a sequence, modeled all the pointing (slewing to and tracking targets) throughout an entire sequence, and modeled all flight rules that relate to spacecraft attitude (including the position of the sun and other celestial bodies). KPT emulated key AACS flight software but ran about 500 times faster than real time, allowing rapid verification of the 10 week background sequence [38].

Significant resources were devoted to validation and verification of each ground software tool. This verification effort was especially intense prelaunch and during the 6.7 year cruise to Saturn. Even during the orbital mission at Saturn, many tools required extensive updates or fixes. Each ground software tool was configuration-controlled by the project, and upgrades and fixes required project manager approval.

An important element of ground software was clear visibility of all flagged violations. KPT produced a violation summary report in a tabular format. This report documented all violations and when they occur, and it listed the science request in effect at the time of the violation. The KPT output log file was also important. This file should document all input and output files as well as include clear details about what caused each violation. The KPT log file needs to give the analyst as much visibility as possible into what led to each violation.

Engineers must have confidence in the ground software tools they use. Configuration control is vital, especially making sure that outdated versions of ground software cannot be accidentally invoked by analysts. Just as important is to ensure that ground software does not incorrectly flag a violation. Real violations may be ignored if the analyst notes that the tool is flagging violations incorrectly.

XII. Operational Lessons Learned: Avoiding Human Error

Avoiding human error in spacecraft operations is a vital aspect of mission success but is often overlooked when a mission's detailed requirements and capabilities are established [66]. Many space missions have been degraded, or ended, due to human error during operations. In any long-duration mission, ground engineers or controllers will sometimes make mistakes, perhaps just through complacency. The goal is to establish a mission operations system, meaning an operations team and their tools and processes, that identifies and corrects mistakes before any incorrect commanding reaches the spacecraft.

The Cassini spacecraft was designed to be fault-tolerant and robust. Great care was taken in building the spacecraft so that the computers, propellant tanks and lines, sensors, and actuators would last for at least a decade, and hopefully much longer. The design of the AACS flight software also aided operators: for example, it rejected any command to power off a required resource (for example, the prime IRU). The design also provided good visibility of spacecraft states. This is key in regular operations and is especially important if an anomaly causes autonomous fault protection action. On Cassini, a large dedicated buffer in the AFC, called the fault protection event log, contained the entire history, with time tags, of any onboard fault response. This kind of visibility greatly aided in understanding the root cause of a spacecraft anomaly.

Some mistakes can occur because the ground controller does not follow a procedure correctly. Others can occur because there is no documented procedure at all. Sometimes, an experienced engineer will go on vacation and not have an adequately trained backup. Other times, a new engineer will come onboard and make a mistake that no one detects. The Cassini AACS operations team provided formal and informal tutorials to new AACS engineers to help them learn about the flight hardware and software, how the spacecraft was commanded, and details about telemetry visibility. A new analyst became acquainted with key ground software tools and processes to build and validate command sequences. Adequate training, having an experienced backup to check all flight products, regularly scheduled peer reviews of each command sequence product, and not rushing through a verification process to meet a deadline, all these and more need to be a part of standard operating procedure.

An important way to track down and fix a human error is to test a spacecraft command sequence on the ground before it is uplinked to the spacecraft. Either the ITL [61–63] or the FSDS [51–53] test bed mentioned in Sec. XI would normally detect any error in a command sequence. The authors are aware of two missions in which tests were performed and violations in the form of plots were generated, but ground operators missed the violation because the simulation outputs did not clearly highlight the violations. The sequence was uplinked and the spacecraft went into safe mode as a result. Violations must be clearly flagged in the test report.

Besides having fully capable tools, human error is more likely to creep in when an engineer is not given enough time to complete the given task, does not adequately understand the task, does not follow a clear procedure, or does not review his/her verification results carefully enough or with others. Peer reviews were added as a standard review step for all future sequences. At the peer review, the entire AACS team reviews all the verification results that the lead AACS analyst for a particular science sequence has performed. The informal nature of these meetings is conducive to asking questions and allowing each engineer to learn in detail about issues that inevitably are relevant to their own lead responsibilities, too.

Because absences or sickness could happen anytime, fully capable "backup" engineers shadowed the lead Cassini AACS engineer for all background and OTM sequence design and verification. These backups were a crucial additional set of "eyes" because everyone at some point overlooks a parameter value or could miss a procedural step. The backup engineer was especially important when the lead AACS analyst for a sequence was relatively inexperienced.

The Cassini team also used detailed checklists for sequence verification that included sanity checks along with formal flight rules.

A different checklist was used for OTMs or other real-time activities. These checklists evolved from previous experience where an analyst may have made a mistake, and so checklists were key in alerting an analyst to areas of potential human error that require extra care. Both the lead and backup engineers should participate in checklist completion [44].

XIII. Attitude Control Fault Protection Operations

The architecture of the FP flight software algorithms that perform autonomous detection, isolation, and recovery from failures of AACS equipment and AACS-controlled propulsion elements is described in [31]. The front end of this architecture was a set of error monitors. Error monitors tested the performance of AACS sensors, actuators, or functions (e.g., attitude estimation) against expectations. Deviations between the actual and expected performance were gauged against a preselected set of "thresholds". An error monitor was "triggered" if its threshold was exceeded for a time duration that was longer than a persistence limit. Prelaunch, both the thresholds and persistence limits of all the error monitors were carefully selected by a team of FP engineers using ground-based test results. Flight experience indicated that most of these parameters were well selected, but some thresholds and persistence limits must be changed in flight because of anomalous sensor performance experienced postlaunch [1,30–36].

The Cassini AACS FP design contains more than 400 error monitors. Not all error monitors are active during a particular spacecraft activity, but a large number of them are. The performance of these active error monitors must be monitored even if none of them are triggered. This is because one or more "untriggered" error monitors might be a "hair line" away from being triggered. To monitor the performance of these error monitors, the "high water marks" (HWMs) of the error monitors are computed by the FSW and sent down as telemetry. To efficiently gauge the performance of hundreds of error monitors, we first convert the HWM data into percentages of their respective thresholds. Computed values of these "percentages" are then displayed graphically (see Fig. 5). One glance at this plot will provide the AACS FP engineer with a quick assessment of the FP performance. For example, from Fig. 5, we see that the threshold of the error monitor named "IRU parity violation" error monitor has been violated.

Selecting the thresholds and persistence limits of error monitors involved compromises. If the threshold was set too low, the monitor would be triggered even when there is not any problem. This is a "false alarm" scenario. On the other hand, if the threshold was set too high, an abnormality might escape detection when a FP response is warranted. This is a "missed detection" scenario. In flight, the AACS FP team used the graphical tool described previously to gauge whether the thresholds and persistence limits selected prelaunch represent good compromises. If the threshold of an error monitor was poorly selected prelaunch, one will see that the value of percentage quantity will always hover near 90–100%. A revision of the threshold might then be necessary [67].

XIV. Spacecraft Commanding and Safe Mode

Cassini was designed to accomplish science and engineering activities using stored sequences of commands. Sequences are time-ordered sets of commands that are recognized by the onboard flight computers. Each command has a time tag, and that command was issued at that time. In practice, a sequence began at a specific UTC (Coordinated Universal Time, onboard UTC is called SCET for spacecraft event time) and each subsequent command was sequenced a given number of integer seconds after the previous command is issued. Each background sequence spanned about 10 weeks. The ground team usually built a background sequence about five months before it was uplinked to the spacecraft. If sequence S98 was executing onboard, sequence S99 was uplinked about one week before the end of S98 so that it was resident and ready to execute when S98 finished. In parallel, the ground team was preparing sequence S100 and was planning S101.

Minisequences and other real-time commands were designed for activities that could not accommodate a five-month background sequence lead time. These smaller sets of commands were also time-ordered and ran in parallel with an onboard background sequence. For example, the S98 background sequence may issue a command to turn the spacecraft to Earth-point at time T0. The turn takes 10 min, and when complete the spacecraft is tracking the Earth until another command is issued to begin a roll about the HGA axis at $T0 + 30$ min. The roll finishes at $T0 + 4$ h. A ΔV maneuver minisequence is uplinked at $T0 + 30$ min and reaches the spacecraft at $T0 + 2$ h. This minisequence will begin executing at $T0 + 5$ h by

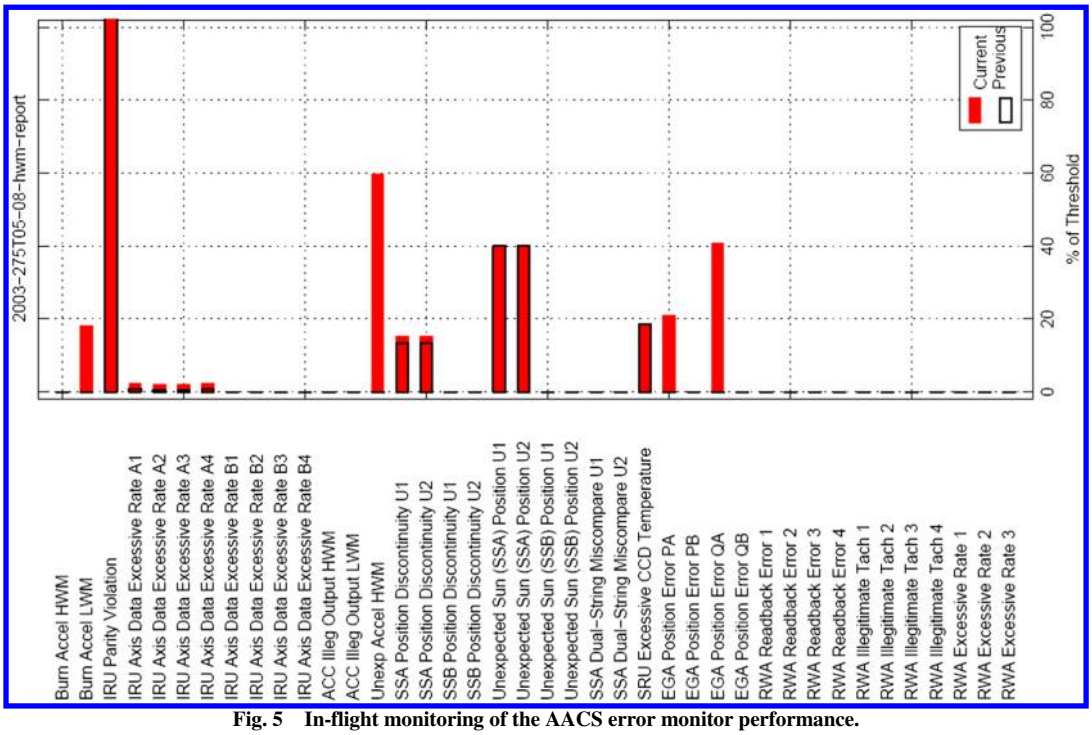

Fig. 5 In-flight monitoring of the AACS error monitor performance.

warming up the accelerometer. It commands main engine burn ignition at $T0 + 6$ h. Both the background sequence and the ΔV minisequence are running concurrently and care must be taken that they do not clash. An even smaller real-time command file could be uplinked at $T0 + 1$ h to specify downlink data rates after the maneuver is complete. All three sequences can run concurrently.

To meet the "fail safe" requirement, Cassini FP design will autonomously locate and isolate any single failure and recover to a thermally safe and commandable attitude on thruster control. This process is called a "safe mode" event. If safe mode is triggered, all stored sequences stop executing. Cassini autonomously turns to the "nominal" safe mode attitude [36]. An onboard "safe table" contains the pointing vectors that define the safe mode attitude. This table can be changed via sequenced command.

When Cassini was in the inner solar system, the nominal safe mode attitude was: NEG_Z to SUN (primary body and inertial vectors), POS_X to J2000Z (secondary body and inertial vectors). This insured both commandability through an onboard low-gain antenna and a thermally safe spacecraft. To achieve downlink through the HGA (In Table 1, the HGA pointing control requirement is 3.2 mrad), a command to change from sun-pointed to Earth-pointed attitude must be sent. In 2003, ground controllers uplinked a new flight software load that updated the onboard safe mode fault response. The new safe mode response still began by commanding the nominal sun-pointed safe mode attitude, but after 60 min, a switch to the Earth-pointed attitude was executed autonomously. This allowed ground controllers to more rapidly assess and respond to the spacecraft anomaly that triggered the safing event.

A complete list of safing events of the Cassini mission is given in Table 2. In that table, safing events 1, 2, and 2a were caused by anomalous AACS performance. Safing events 3 and 4 were caused by operator errors. Safing events 5 and 6 were due to the impacts of cosmic ray on electronic devices. In 20 years (1997–2017), Cassini put itself into safe mode six times. Considering the complexity of demands the mission operation team had to make on Cassini, the spacecraft performed exceptionally well. This record supports the claim that the spacecraft was well designed and the Cassini Spacecraft Operations (SCO) team was well trained. Many members of the SCO team were with the project since before launch. Their knowledge and training enabled quick recoveries from safe mode and rapid resumption of the nominal mission.

XV. Avoid Changing Flight Software by Patching

One way that human error in operations can adversely affect a spacecraft is by changing flight software without sufficient rigor. Mars Global Surveyor encountered this in 2006 [69]. Flight software configuration management on Cassini had been strictly followed throughout the mission. A formal process involving project manager approval was required to even begin the effort to make a change to the flight software source code. Then, extensive ITL and FSDS regression testing demonstrated that the change had no adverse impact on any operational scenario. Testing had to clearly show the "before" and "after" effect of any change. Then, procedures and command sequences were generated and successfully executed in ITL to demonstrate that the process of uplinking and loading the FSW was seamlessly integrated with the onboard background sequence. Only after all these checks are passed did the project manager permit the flight software change to be made onboard.

The AACS FSW version that was used at launch was called A6.3.5. Consistent with the plan made at the time of launch, the AACS FSW was updated with new versions several times during the long cruise phase and during the early tour phase. A summary of all full-load FSW updates is given in Table 3 [70]. In Table 3, both A8.7.1 and A8.8.0 were full FSW loads. In between them, there were five patch loads: A8.7.2, A8.7.4, A8.7.5, A8.7.6, and A8.7.7 [34]. The full load A8.8.0 was based on patches introduced by A8.7.2 to A8.7.7. Human error can occur if a small "patch" to the flight software is introduced. The normal way ground controllers command the flight computer is via goal-oriented sequence commands. Sequence commands have built-in checks to ensure that commands are not corrupted. They also have mode and range checks. If an operator makes an error in a command argument, the flight computer will reject the command. On Cassini, the spacecraft mass properties, thrust characteristics, and many other parameter changes all used standard commands with full parsing, handshake, and validity checks. Memory write commands (patches) bypass most of these checks. That is why patching via memory write was discouraged on Cassini.

In the rare case that a patch command must be used, the AACS team had to follow the same rigorous process of testing and project approval as for a full flight software upload. Cassini experience showed that any direct patch to the FSW RAM should only change a

Table 2 Cassini safing events, October 1997–September 2017

Safing	Date	Root cause(s)
1	1998-DOY-083	A swap of tracker triggered a "large Z/σ ratio"[a] monitor.
2	1999-DOY-012	Slow roll tripped a large Z/σ ratio[a] error monitor.
2a	2000-DOY-350	Low-rpm RWA operation led to high bearing drag. A triggered error monitor caused a RWA-to-RCS transition without calling safing. Subsequent science mosaic slews on thrusters wasted hydrazine.
3	2001-DOY-130	Caused by a CDS configuration management error. Root cause is "operator error".
4	2003-DOY-132	Missing an inertial vector table target vector. Root cause is operator error.
5	2007-DOY-254	SSPS (solid-state power switch) of TWTA-B line was tripped off. Cosmic ray hit.
6	2010-DOY-307	File corruption causing swap from CDS-A to B. Cosmic ray hit.

[a]In between star tracker measurement updates, S/C attitude estimate is updated using the IRU data. In the flight software, the propagated attitude estimate is compared with the tracker measurement update, and an error residual vector (called "z") is computed. If z is unreasonably large relative to the estimation uncertainty of the extended Kalman–Bucy filter (called "σ"), an anomalous tracker and/or gyroscope performance might have occurred.

Table 3 Cassini AACS full-LOAD FSW updates and patches [44,70]

FSW	Date uploaded	Key FSW capabilities added
A6.3.5	15 Oct. 1997	Launch load
A7.7.6	7 March 2000	Detect thruster leak during long cruise [33]; enhanced RWA control performance [18]; enhanced SID algorithm to handle extended bodies in tracker's FOV; "deluxe" attitude initialization capability (for SOI); IVP with rotating coordinates (probe tracking); gyroless attitude estimation capability.
A8.6.5	16 Feb. 2003	This is the load used by TCM-19b as an in-flight confirmation of the "energy-based" burn termination algorithm (for SOI) [22].
A8.6.7	27 April 2004	This is the load for SOI burn. All SOI-related RCS slews were checked with this load. Confirmations of FSW capability to autonomously disable six SSA error monitors using the eclipse command and to propagate attitude with long-duration SID suspend.
A8.7.1	2 Oct. 2004	This is the load for probe release and probe relay [37]. Parameter updates for probe release and relay. Reference trajectory updates for probe relay.
A8.8.0	22 Oct. 2010	FSW changes include RWA safing design, fixes to telemetry channels, updated thruster magnitudes, tracker misalignment matrix, AACS recovery data, and active RAM patches.
A8.9.0	12 Dec. 2012	FP design to handle B-thruster leak in a mixed-branch RCS control configuration, updates to default safing attitude, default thruster magnitude, mass properties, CMT acceleration limit, and active RAM patches. This is the last FSW upload.

variable, not an instruction or a constant. Patching an instruction or a constant will change the FSW checksum. This is to be avoided because, if a flight computer reset were to occur, this checksum must match the original FSW image checksum, otherwise the AFC would not progress from ROM to RAM. In February of 2003, this did happen once in flight (to the backup AFC) during a planned FSW upload. The problem was traced to the patching of a constant before 2003 that altered the FSW checksum. After this event, a flight rule was created to always use the AFC and SSR (solid-state recorder) "patch table" (limited to 304 words) if a constant or instruction needs to be changed. The patch table method was robust and ensured a consistent checksum, a new FSW version number, and smooth progression into normal RAM operation, as well as preservation of the patched parameters after a flight computer reset [44].

XVI. Estimations of Titan and Enceladus Atmospheric Densities

The Cassini spacecraft attitude was controlled by RCS thrusters during all low-altitude (less than 1300 km) Titan flybys. Thrusters were fired to overcome torque imparted on the spacecraft due to Titan atmosphere as well as to slew the spacecraft to meet the pointing needs of science instruments. Obviously, the denser that Titan's atmosphere was, the more thruster firings were needed. Thus, thruster firing telemetry data were used to estimate the three per-axis torques imparted on the spacecraft due to Titan's atmosphere. Titan atmospheric density (as a function of altitude) could be estimated from the computed time-varying atmospheric torque if we knew the spacecraft velocity relative to Titan, the projected area of the spacecraft on a plane perpendicular to the velocity vector, the offset distance between the S/C's c.m. and center of pressure, and the drag coefficient. Details of this methodology are given in [2,71–76]. The one-sigma estimated uncertainty of the computed atmospheric density is 6% [72,73]. In 2005–2013, this methodology was applied on attitude control telemetry data from 48 low-altitude Titan flybys executed [73,74]. In 2006, aerothermodynamics studies of two Cassini Titan flybys, Titan-A and Titan-5, were conducted using the direct simulation Monte Carlo methodology [77]. These studies reported torque imparted on the spacecraft that agreed to within 15% of those reported by the Cassini AACS team. This was an independent verification of the results reported by the Cassini AACS team. Density estimates made using AACS data provided the Cassini project with a wealth of Titan atmospheric density data that were used to calibrate INMS-based density estimate [39]. This was a significant contribution that the AACS team made to the attainment of a key Cassini science objective. A similar approach was used to estimate the Enceladus plume density [2,75].

XVII. Conclusions

A sophisticated interplanetary spacecraft, Cassini–Huygens, was launched on 15 October 1997 and arrived at Saturn on 30 June 2004. Over the entire mission (1997–2017), the flight performance of the Cassini attitude and articulation control subsystem was superb. All key mission and science pointing accuracy requirements were met with significant margins. Details of the Cassini AACS designs and flight performance are documented in more than 97 papers published in 1992–2018. These papers capture calibration results of the S/C's inertia matrix [78], trends of gyroscopes' scale factor and misalignment [10–12], trends of RWA bearing drag torque [12,13,41,46], propellant slosh frequencies [79,80], sun sensor performance [1,12,81], and thrusters' magnitude and response time [12,15,49,50]. Atmospheric densities of Titan [71–74,76], Enceladus [2,75], and Saturn [5] that were estimated using AACS flight data had already been used to supplement results collected by Cassini science instruments [39]. Over the last five months of the mission (from 23 April to 15 September 2017), Cassini sent back new science data from 22 proximal orbits before the mission ended on 15 September 2017 [4,5,82]. AACS-centric lessons learned from two decades of Cassini mission operations are documented in this paper. Some of these lessons learned could be equally applicable to the safe operation of other missions.

Acknowledgments

The work described in this paper was carried out by the Jet Propulsion Laboratory, California Institute of Technology, under contract with NASA. We wish to thank our colleagues David M. Bates and Todd Brown for their reviews of an earlier version of this paper. The encouragement and support of Julie L. Webster is also acknowledged. We also want to thank the Associate Editor and the anonymous reviewers for their valuable and constructive comments on the submitted journal version of this paper.

References

[1] Lee, A. Y., and Hanover, G., "Cassini Spacecraft Attitude Control System Flight Performance," *AIAA Guidance, Navigation, and Control Conference and Exhibit*, AIAA Paper 2005-6269, Aug. 2005.

[2] Lee, A. Y., Wang, E. K., Pilinski, E. B., Macala, G. A., and Feldman, A., "Estimation and Modeling of Enceladus Plume Jet Density Using Cassini Flight Data," *Journal of Spacecraft and Rockets*, Vol. 50, No. 2, March–April 2013, pp. 317–325.

[3] Burk, T. A., "Cassini at Saturn Proximal Orbits–Attitude Control Challenge," *AIAA Guidance, Navigation, and Control Conference*, AIAA Paper 2013-4710, Aug. 2013.

[4] Sung, T. S., "Cassini's Grand Finale–Attitude Control Subsystem Performance During Proximal Ring Plane Crossings," *2018 AIAA Guidance, Navigation, and Control Conference*, AIAA Paper 2018-2022, Jan. 2018.

[5] Andrade, L. G., "Skimming Through Saturn's Atmosphere: The Climax of the Cassini Grand Finale Mission," *2018 AIAA Guidance, Navigation, and Control Conference*, AIAA Paper 2018-2111, Jan. 2018.

[6] Thomas, V. C., Alexander, J. A., Dennison, E. W., Waddell, P. G., Borghi, G., and Procopio, D., "Cassini Star Tracking and Identification Architecture," *SPIE*, Vol. 2221, July 1994, pp. 288–298.

[7] Alexander, J. W., and Chang, D. H., "Cassini Star Tracking and Identification Algorithms, Scene Simulation, and Testing," *SPIE*, Vol. 2803, 1996, pp. 311–336.

[8] Lee, A. Y., "Risk Assessment of Hypervelocity Impact of Saturn Dust on Cassini Sun Sensors," *Journal of Spacecraft and Rockets*, Vol. 54, No. 2, March–April 2017, pp. 417–425.

[9] Litty, E. C., Gresham, L. L., Toole, P. A., and Beisecker, D. A., "Hemispherical Resonator Gyroscope: An IRU for Cassini," *SPIE*, Vol. 2803, Oct. 1996, pp. 299–310.

[10] Burrough, E. L., and Lee, A. Y., "In-Flight Characterization of the Cassini Spacecraft's Inertial Reference Units," *AIAA Guidance, Navigation, and Control Conference*, AIAA Paper 2007-6340, Aug. 2007.

[11] Brown, T., "In-Flight Performance of the Cassini Hemispherical Quartz Resonator Gyro Inertial Reference Units," *AIAA Guidance, Navigation, and Control Conference*, AIAA Paper 2013-4630, Aug. 2013.

[12] Stupik, J., "Mission Summary of Cassini Spacecraft Guidance and Control Hardware Health and Performance," *2018 AIAA Guidance, Navigation, and Control Conference*, AIAA Paper 2018-2110, Jan. 2018.

[13] Lee, A. Y., and Wang, E. K., "Inflight Performance of Cassini Reaction Wheel Bearing Drag in 1997–2013," *Journal of Spacecraft and Rockets*, Vol. 52, No. 2, March–April 2015, pp. 470–480.

[14] Barber, T. J., and Cowley, R. T., "Initial Cassini Propulsion System In-Flight Characterization," *38th AIAA/ASME/SAE/ASEE Joint Propulsion Conference and Exhibit*, AIAA Paper 2002-4152, July 2002.

[15] Bates, D., and Lee, A. Y., "In-Flight Characterization of the Cassini Spacecraft Attitude Control Thrusters," *AIAA Guidance, Navigation, and Control Conference and Exhibit*, AIAA Paper 2007-6342, Aug. 2007.

[16] Burk, T. A., "Extended Bright Bodies–Flight and Ground Software Challenges on the Cassini Mission at Saturn," *AIAA Guidance, Navigation, and Control Conference*, AIAA Paper 2016-2090, Jan. 2016.

[17] Wong, E., and Breckenridge, W., "An Attitude Control Design for the Cassini Spacecraft," *Guidance, Navigation, and Control Conference*, AIAA Paper 1995-3274, 1995.

[18] Macala, G. A., "Design of the Reaction Wheel Attitude Control System for the Cassini Spacecraft," *AAS/AIAA Space Flight Mechanics Meeting*, American Astronautical Soc. Paper 02-121, Springfield, VA, Jan. 2002.

[19] Lee, C., and Lee, A. Y., "Cassini Reaction Wheel Momentum Bias Optimization Tool," *AIAA Guidance, Navigation, and Control Conference and Exhibit*, AIAA Paper 2005-6271, Aug. 2005.
[20] Enright, P. J., "Attitude Control of the Cassini Spacecraft During Propulsive Maneuvers," *AAS/AIAA Astrodynamics Specialist Conference*, American Astronautical Soc. Paper 93-552, Springfield, VA, Aug. 1993.
[21] Enright, P. J., "Thrust Vector Control Algorithm Design for the Cassini Spacecraft," *AIAA/AHS/ASEE Aerospace Design Conference*, AIAA Paper 1993-1043, Feb. 1993.
[22] Lam, D. C., Friberg, K. H., Brown, J. M., Sarani, S., and Lee, A. Y., "An Energy Burn Algorithm for Cassini Saturn Orbit Insertion," *AIAA Guidance, Navigation, and Control Conference and Exhibit*, AIAA Paper 2005-5994, Aug. 2005.
[23] Burk, T. A., "Attitude Control Performance During Cassini Trajectory Correction Maneuvers," *AIAA Guidance, Navigation, and Control Conference and Exhibit*, AIAA Paper 2005-6270, Aug. 2005.
[24] Burk, T. A., "Cassini Orbit Trim Maneuvers at Saturn–Overview of Attitude Control Flight Operations," *AIAA Guidance, Navigation, and Control Conference*, AIAA Paper 2011-6549, Aug. 2011.
[25] Rasmussen, R. D., Singh, G., Rathbun, D. B., and Macala, G. A., "Behavioral Model Pointing on Cassini Using Target Vectors," *Annual Rocky Mountain Guidance and Control Conference*, The International Soc. for Optical Engineering, Feb. 1995, pp. 91–110; also *SPIE*, Vol. 2803, pp. 271–287.
[26] Burk, T. A., "A Cassini Pointing Operations Flight Experience Using Inertial Vector Propagation," *AIAA Guidance, Navigation, and Control Conference and Exhibit*, AIAA Paper 2007-6339, Aug. 2007.
[27] Goodyear, W. H., "Completely General Closed-Form Solution for Coordinates and Partial Derivatives of the Two-Body Problem," *Astronomical Journal*, Vol. 70, No. 3, April 1965, pp. 189–192.
[28] Barrodale, I., and Phillips, C., "Algorithm 495. Solution of an Overdetermined System of Linear Equations in the Chebyshev Norm," *ACM Transactions on Mathematical Software*, Vol. 1, No. 3, Sept. 1975, pp. 264–270.
[29] Singh, G., Macala, G. A., Wong, E. C., and Rasmussen, R. D., "A Constraint Monitor Algorithm for the Cassini Spacecraft," *Guidance, Navigation, and Control Conference*, AIAA Paper 1997-3526, Aug. 1997.
[30] Brown, G. M., Bernard, D. E., and Rasmussen, R. D., "Attitude and Articulation Control for the Cassini Spacecraft: A Fault Tolerance Overview," *14th AIAA/IEEE Digital Avionics System Conference*, IEEE Publ., Piscataway, NJ, Nov. 1995.
[31] Brown, G. M., and Johnson, S. A., "An Overview of the Fault Protection Design for the Attitude Control Subsystem of the Cassini Spacecraft," *American Control Conference*, IEEE Publ., Piscataway, NJ, June 1998.
[32] Meakin, P. C., "Cassini Attitude Control Fault Protection: Launch to End of Prime Mission Performance," *AIAA Guidance, Navigation, and Control Conference and Exhibit*, AIAA Paper 2008-6809, Aug. 2008.
[33] Lee, A. Y., "Model-Based Thruster Leakage Monitor for the Cassini Spacecraft," *Journal of Spacecraft and Rockets*, Vol. 36, No. 5, Sept.–Oct. 1999, pp. 745–749.
[34] Cooney, L. A., "Cassini Attitude Control Fault Protection: Flight Operations Strategy Changes for Extended Mission," *AIAA Guidance, Navigation, and Control Conference*, AIAA Paper 2010-7561, Aug. 2010.
[35] Bates, D. M., "Cassini Attitude and Articulation Control Subsystem Fault Protection Challenges During Saturn Proximal Orbits," *AIAA Guidance, Navigation, and Control Conference*, AIAA Paper 2015-0077, Jan. 2015.
[36] Burk, T. A., "Managing Cassini Safe Mode Attitude at Saturn," *AIAA Guidance, Navigation, and Control Conference*, AIAA Paper 2010-7558, Aug. 2010.
[37] Allestad, D. L., Standley, S. P., Chang, L., and Bone, B. D., "Systems Overview of the Cassini–Huygens Probe Relay Critical Sequence," *AIAA Guidance, Navigation, and Control Conference and Exhibit*, AIAA Paper 2005-6388, Aug. 2005.
[38] Burk, T. A., and Bates, D. M., "Cassini Attitude Control Operation: Flight Rules and How They Are Enforced," *AIAA Guidance, Navigation, and Control Conference and Exhibit*, AIAA Paper 2008-6808, Aug. 2008.
[39] Teolis, B. D., Niemann, H. B., Waite, J. H., Gell, D. A., Perryman, R. S., Kasprzak, W. T., Mandt, K. E., Yelle, R. V., Lee, A. Y., and Pelletier, F. J., et al., "A Revised Sensitivity Model for Cassini INMS: Results at Titan," *Space Science Reviews*, Vol. 190, No. 1, July 2015, pp. 47–84.
[40] Brown, T., "In-Flight Tuning of the Cassini RCS Attitude Controller," *AIAA Guidance, Navigation, and Control Conference*, AIAA Paper 2011-6550, Aug. 2011.
[41] Lee, A. Y., "Performance of Cassini Reaction Wheel Friction Compensation Scheme During Spin Rate Zero-Crossing and Drag Spikes," *2018 AIAA Guidance, Navigation, and Control Conference*, AIAA Paper 2018-2112, Jan. 2018.
[42] Pilinski, E., and Lee, A. Y., "Pointing Stability Performance of the Cassini Spacecraft," *Journal of Spacecraft and Rockets*, Vol. 46, No. 5, Sept.–Oct. 2009, pp. 1007–1015.
[43] Lucke, R. L., Sirlin, S. W., and San Martin, A. M., "New Definitions of Pointing Stability: AC and DC Effects," *Journal of Astronautical Sciences*, Vol. 40, No. 4, 1992, pp. 557–576.
[44] Lee, A. Y., and Burk, T. A., "Cassini Spacecraft Attitude Control System Flight Performance and Lessons Learned, 1997–2017," *2018 AIAA Guidance, Navigation, and Control Conference*, AIAA Paper 2018-2109, Jan. 2018.
[45] Mittelsteadt, C. O., "Cassini Attitude Control Operations–Guidelines Levied on Science to Extend Reaction Wheel Life," *AIAA Guidance, Navigation, and Control Conference*, AIAA Paper 2011-6553, Aug. 2011.
[46] Brown, T. S., "The Cassini Reaction Wheels: Drag and Spin-Rate Trends from an Aging Interplanetary Spacecraft at Saturn," *AIAA Guidance, Navigation, and Control Conference*, AIAA Paper 2016-2085, Jan. 2016.
[47] Macala, G. A., Lee, A. Y., and Wang, E. K., "Feasibility Study of Two Candidate Reaction Wheel/Thruster Hybrid Control Architecture Designs for the Cassini Spacecraft," *Journal of Spacecraft and Rockets*, Vol. 51, No. 2, March–April 2014, pp. 574–585.
[48] Smith, B. A., Lim, R. S., Feldman, A., and Salami, M., "Dawn Spacecraft Performance at Ceres: Results of Hybrid Controller for Ceres Mapping," *AAS Guidance and Control Conference*, American Astronautical Soc. Paper 17-151, Springfield, VA, Feb. 2017.
[49] Feldman, A., and Lee, A. Y., "In-Flight Estimation of Cassini Spacecraft Inertia Tensor and Thruster Magnitude," *AAS/AIAA Space Flight Mechanics Meeting*, American Astronautical Soc. Paper 06-102, Springfield, VA, Jan. 2006.
[50] Stupik, J., and Burk, T. A., "Thruster-Specific Force Estimation and Trending of Cassini Hydrazine Thrusters at Saturn," *AIAA Guidance, Navigation, and Control Conference*, AIAA Paper 2016-2087, Jan. 2016.
[51] Brown, J. M., Lam, D., Burk, T. A., and Wette, M., "The Role of the Flight Software Development System Simulator Throughout the Cassini Mission," *AIAA Guidance, Navigation, and Control Conference and Exhibit*, AIAA Paper 2005-6389, Aug. 2005.
[52] Wang, E. K., and Brown, J., "Cassini Test Methodology for Flight Software Verification During Mission Operations," *AIAA Guidance, Navigation, and Control Conference*, AIAA Paper 2007-6341, Aug. 2007.
[53] Brown, J., Wang, E. K., Hernandez, J., and Lee, A. Y., "Importance of Model Simulations in Cassini In-Flight Mission Events," *AIAA Guidance, Navigation, and Control Conference*, AIAA Paper 2009-5762, Aug. 2009.
[54] Ardalan, S. M., Antreasian, P. G., Criddle, K. E., Ionasescu, R., Jacobson, R. A., Jones, J. B., MacKenzie, R. A., Parcher, D. W., Pelletier, F. J., and Roth, D. C., et al., "Integration of Spacecraft Telemetry into Navigation Operations for the Cassini–Huygens Mission," *SpaceOps 2008 Conference*, AIAA Paper 2008-3412, 2008.
[55] Brown, T., "Y-Biasing: A New Operational Method for Cassini to Control Thruster Usage While Managing Reaction Wheel Momentum," *AIAA Guidance, Navigation, and Control Conference*, AIAA Paper 2010-7560, Aug. 2010.
[56] Velarde Yang, G., Kirby, C., and Mohr, D., "Cassini's Maneuver Automation Software Process: How to Successfully Command 200 Navigation Maneuvers," *AIAA Guidance, Navigation, and Control Conference and Exhibit*, AIAA Paper 2008-6807, Aug. 2008.
[57] Wagner, S., "Cassini Maneuver Performance Assessment and Execution-Error Modeling Through 2015," *AAS/AIAA Space Flight Mechanics Meeting*, American Astronautical Soc. Paper 16-305, Springfield, VA, Feb. 2016.
[58] Brown, T. S., "A Full Mission Summary (1997–2017) of the Attitude Control Performance During Orbit Trim Maneuvers Performed by the Cassini–Huygens Spacecraft," *2018 AIAA Guidance, Navigation, and Control Conference*, AIAA Paper 2018-2023, Jan. 2018.
[59] Smith, B. A., "Three Year Orbital Trim Maneuver Performance of the Cassini Spacecraft Attitude Control Subsystem," *31st Annual AAS Guidance and Control Conference*, American Astronautical Soc., Springfield, VA, Feb. 2008, Paper 08-0101.
[60] Bates, D. M., "Cassini Spacecraft In-Flight Swap to Backup Attitude Control Thrusters," *AIAA Guidance, Navigation, and Control Conference*, AIAA Paper 2010-7559, Aug. 2010.
[61] Mizukami, M., Barber, T. J., Christodoulou, L. N., Guernsey, G. S., and Haney, W. A., "Cassini Spacecraft Reaction Control System Thrusters Flight Experience," *JANNAF Propulsion Meeting*, Colorado Springs, CO, May 2010.

[62] Badaruddin, K., Hernandez, J., and Brown, J., "The Importance of Hardware-in-the-Loop Testing to the Cassini Mission to Saturn," *IEEE Aerospace Conference*, IEEE Publ., Piscataway, NJ, March 2007, Paper 1231.

[63] Cervantes, D., Badaruddin, K., and Huh, S. M., "Integrated Testing of the Saturn Orbit Insertion Critical Sequence," *AIAA Guidance, Navigation, and Control Conference and Exhibit*, AIAA Paper 2005-6272, Aug. 2005.

[64] Montañez, L., Bone, B. D., and Laufer, P., "Evolution of the Cassini Attitude and Articulation Control Subsystem Simulation During a Seven-Year Cruise Mission Phase," *AIAA Guidance, Navigation, and Control Conference and Exhibit*, AIAA Paper 2005-6273, Aug. 2005.

[65] Chang, L., Brown, J., Barltrop, K., and Lee, A. Y., "Use of Guidance and Control Test Cases to Verify Spacecraft Attitude Control System Design," *12th AAS/AIAA Spaceflight Mechanics Meeting*, American Astronautical Soc. Paper 02-123, Springfield, VA, Jan. 2002.

[66] Burk, T., "Avoiding Human Error in Mission Operations: Cassini Flight Experience," *AIAA Guidance, Navigation, and Control Conference*, AIAA Paper 2012-4607, Aug. 2012.

[67] Bates, D., Lee, A. Y., Meakin, P., and Weitl, R., "Fault Protection Design and Testing for the Cassini Spacecraft in a Mixed Thruster Configuration," *AIAA Guidance, Navigation, and Control Conference*, AIAA Paper 2013-4632, Aug. 2013.

[68] Sung, T., and Burk, T., "Extended Bright Bodies–Flight and Ground Software Challenges on the Cassini Mission at Saturn," *AIAA Guidance, Navigation, and Control Conference*, AIAA Paper 2016-2090, Jan. 2016.

[69] Perkins, D., "Mars Global Surveyor Spacecraft Loss of Contact," Mars Global Surveyor White Paper, Jet Propulsion Laboratory, April 2007.

[70] Brown, J., "Cassini Attitude Control Flight Software: From Development to In-Flight Operation," *AIAA Guidance, Navigation, and Control Conference and Exhibit*, AIAA Paper 2008-6806, Aug. 2008.

[71] Feldman, A., Brown, J. M., Wang, E. K., Peer, S. G., and Lee, A. Y., "Reconstruction of Titan Atmosphere Density Using Cassini Attitude Control Flight Data," *AAS/AIAA Space Flight Mechanics Meeting*, American Astronautical Soc. Paper 07-187, Springfield, VA, Jan.–Feb. 2007.

[72] Sarani, S., "Titan Atmospheric Density Reconstruction Using Cassini Guidance, Navigation, and Control Data," *AIAA Guidance, Navigation, and Control Conference*, AIAA Paper 2009-5763, Aug. 2009.

[73] Lee, A. Y., and Lim, R. S., "Evidence of Temporal Variation of Titan Atmospheric Density in 2005–2013," *AIAA Guidance, Navigation, and Control Conference*, AIAA Paper 2013-4709, Aug. 2013.

[74] Andrade, L. C., Burk, T. A., and Pelletier, F., "Titan Density Reconstruction Using Radiometric and Cassini Attitude Control Flight Data," *AIAA Guidance, Navigation, and Control Conference*, AIAA Paper 2015-0079, Jan. 2015.

[75] Sarani, S., "Enceladus Plume Density Modeling and Reconstruction for Cassini Attitude Control System," *SpaceOps 2010 Conference*, AIAA Paper 2010-2035, April 2010.

[76] Sarani, S., "A Novel Methodology for Reconstruction of Titan Atmospheric Density Using Cassini Guidance, Navigation, and Control Data," *AIAA Guidance, Navigation, and Control Conference*, AIAA Paper 2007-6343, Aug. 2007.

[77] Liechty, D. S., "Cassini–Huygens Aerodynamics with Comparison to Flight," *25th International Symposium on Rarefied Gas Dynamics*, 2006, Paper 20060047648.

[78] Lee, A. Y., and Wertz, J., "Inflight Calibration of the Cassini Spacecraft Inertia Matrix," *Journal of Spacecraft and Rockets*, Vol. 39, No. 1, Jan.–Feb. 2002, pp. 153–155.

[79] Lee, A. Y., and Stupik, J., "Inflight Characterization of the Cassini Spacecraft Propellant Slosh," *Journal of Spacecraft and Rockets*, Vol. 54, No. 2, March–April 2017, pp. 417–425.

[80] Enright, P., and Wong, E. C., "Propellant Sloshing Models for the Cassini Spacecraft," *Astrodynamics Conference*, AIAA Paper 1994-3730, 1994.

[81] Lim, R. S., "Evaluation of Fuel-Efficient Sun Search Slew Rates for the Cassini Spacecraft in the Cassini Solstice Mission," *AIAA Guidance, Navigation, and Control Conference*, AIAA Paper 2012-4608, Aug. 2012.

[82] Burk, T. A., "Enhanced Reconstructed C-Kernels from Cassini Flight Telemetry at Saturn," *AIAA SciTech*, AIAA Paper 2018-2113, Jan. 2018.

C. W. Roscoe
Associate Editor